Resonant Decay of Finite-Extent Cold-Electron Plasma Waves

K. L. Wong and P. Bellan[a]
Princeton Plasma Physics Laboratory, Princeton, New Jersey 08540

and

M. Porkolab
Department of Physics, Massachusetts Institute of Technology, Cambridge, Massachusetts 02139

(Received 7 November 1977)

The parametric decay of a finite-extent cold-electron plasma wave (slow wave) was studied experimentally. Using a frequency of $\omega_0 \gtrsim 10\omega_{pi}$, it was found that the decay waves propagated along the pump wave rather than in the $\vec{E}_0 \times \vec{B}$ direction. This is in agreement with the recent theoretical predictions of finite-length stabilization.

Radio-frequency heating near the lower-hybrid frequency offers an attractive means to heat fusion plasmas to high temperatures.[1] In order that the externally launched waves penetrate to the plasma interior, two conditions must be met. (1) The electromagnetic waves launched at the plasma periphery must be slowed down by an appropriate slow-wave structure of finite length.[1] (2) There should not be excessive damping of the wave in the outer plasma layers which the wave has to penetrate before reaching the center where $\omega_0 \simeq \omega_{pi}$. Although in high-temperature plasma, collisional damping of the slow wave may not be important, nonlinear effects, such as parametric decay instabilities, may provide unwanted energy deposition in the outer layers.[2-6] In this Letter we report experimental results obtained in a linear plasma device which attempts to study in detail parametric instabilities excited by a finite-extent slow wave at densities such that $\omega_0 \gtrsim 10\omega_{pi}$. Theory predicts that, while in a spatially uniform pump electric field in the regime $\omega_0 \ll \omega_{pe}\omega_{ce}$ the $\vec{E}_0 \times \vec{B}$ forces drive the instability, in a spatially localized pump field (such as expected to be generated in tokamaks) convective losses will greatly reduce the growth rate (unless $1 \lesssim \omega_0/\omega_{LH} < 2$) so that hot-ion plasma waves with small group velocities can be excited.[2,4]

This can be seen as follows. In a magnetized plasma, for $\omega_0 \ll \omega_{pe} \lesssim \omega_{ce}$, the parametric coupling coefficient is given by[3]

$$\mu = \frac{e}{m}\left[\left(\frac{E_{0z}k_z}{\omega_0^2}\right)^2 + \frac{[(\vec{E}_0 \times \vec{k}_\perp)\cdot\hat{z}]^2}{\omega_{ce}^2\omega_0^2}\right]^{1/2}, \quad (1)$$

where ω_{ce} is the electron cyclotron frequency, ω_0 is the pump frequency, and $\vec{B} = B_0\hat{z}$. Here the first term is the parallel drift, and the second term is the $\vec{E}_0 \times \vec{B}$ term. We see that in a uniform pump field, for a slow wave the second term ($\vec{E}_0 \times \vec{k}_\perp$) dominates. Thus, for a radial pump electric field the decay waves should propagate in the azimuthal direction. If the sideband waves are also slow waves (cold-electron plasma waves) then they must satisfy the same dispersion relationship as the pump wave, i.e.,

$$\omega_2 = \frac{k_\parallel}{k}\frac{\omega_{pe}}{(1+\omega_{pe}^2/\omega_{ce}^2)^{1/2}}. \quad (2)$$

Thus, slow waves that propagate mainly in the azimuthal ($\vec{E}_0 \times \vec{B}$) direction will get out of the finite-extent pump-field region (located between resonance cones) and lose amplification. This process sets a relatively high threshold for the excitation of these waves.

To minimize the convective loss, slow waves can propagate along the pump resonance cone and stay inside the pump-field region until they reach the plasma boundary, but this can be driven only by the relatively weak $E_{0z}k_z$ component of Eq. (1) and it requires the sideband frequency to be very close to the pump. Let D be the diameter of the plasma column ($D \sim 10$ cm in our experiment); then the threshold due to the finite-length effect can be estimated by[7]

$$(\gamma_0^2/\gamma_1 - \gamma_2)D/V_{2x} \geq \pi, \quad (3)$$

where V_{2x} is the radial component of the group velocity of the side-band and γ_0 is the growth rate. In a uniform pump field without boundaries, the decay threshold is determined only by the damping rates (γ_1, γ_2) of the decay waves, i.e., $\gamma_0^2 > \gamma_1\gamma_2$. If we keep only the parallel coupling term in Eq. (1) and assume $\omega_{pe}^2 \ll \omega_{ce}^2$, then the collisional threshold is given by

$$E_0 > (2\sqrt{\pi}\, v_{Te} C_s \omega_{pe} \nu_e)^{1/2}(m/e)(\omega_{pe}/\omega_0), \quad (4)$$

where v_{Te} is the electron thermal velcoity, C_s is the ion acoustic speed, ω_{pe} and ω_{ce} are the electron plasma and cyclotron frequencies, and ν_e is

the electron collision frequency ($\sim 1.2\times 10^5$/sec in our experiment). It should be noted that this is the minimum collisional threshold for spatial amplification. However, to obtain sufficient gain, Eq. (3) should be satisfied unless the pump is a standing wave.

In order to test this theory, one must measure the direction of propagation of the decay waves. In the present work, a two-wavelength-long slow-wave structure was used in a nearly uniform plasma, and because of the clean geometry of our system the decay spectrum was very narrow (i.e., $\omega/\omega_0 \simeq 10^{-2}$) and the sideband (electron plasma wave) propagated almost parallel to the pump wave, while the acoustic wave propagated at a large angle to it. We interpret these results as a consequence of the finite-length stabilization of waves propagating in the $\vec{E}_0\times\vec{B}$ direction (i.e., wave propagation in the $\vec{E}_0\times\vec{B}$ direction was not observed). We note that similar parametric decay has been observed in a number of different experiments.[8-14] However, to the best of our knowledge, this is the first experiment with detailed wavelength measurement in all directions which reveals the driving mechanism and confirms the stabilizing effect of convective loss due to the finite extent of the pump field. In some of the previous experiments,[9,10] parametric decay due to $\vec{E}\times\vec{B}$ coupling was observed because of the difference in plasma parameters. $\vec{E}\times\vec{B}$ coupling dominates at large values of $\omega_{pe}^2/\omega_0\omega_{ce}$. Besides, the pump in those experiments was a capacitive electric field excited between metal plates which was different from a propagating electron plasma wave launched from a slow-wave structure.

The experiment was performed in the Princeotn L-3 device with the following parameters: $B\sim 1.3$ kG, $n\sim 2\times 10^{10}/\mathrm{cm}^3$, $T_e\sim 1$–3 eV, $T_i<0.1$ eV. The neutral pressure was 2×10^{-4} Torr and the argon plasma was produced by a multifilament source.[15] The slow waves at $f_0=75$ MHz were launched by a 50-cm-long slow-wave structure,[16] consisting of four alternately phased rings driven by an rf oscillator. Figure 1 shows a schematic of the experimental setup. When the input rf power was increased above a threshold value, parametric decay occurred as shown in Fig. 2(a). From the spectrum, it is apparent that the frequency-matching condition is satisfied. In order to identify the decay waves, the wavelengths were measured by interferometry. The interferograms are shown in Fig. 3(a). The pump wavelength ($\lambda_\perp\sim 1.5$ cm) is about 5 times longer than that of the decay waves. The high- and low-frequency decay waves have nearly equal wavelengths in the radial ($\lambda_\perp\sim 3$ mm) and axial ($\lambda_\parallel\sim 4$ cm) directions, respectively. Azimuthal interferometer measurements made with a rotating azimuthal probe showed that there was no measurable wavelength in the azimuthal direction. A lower bound of $\lambda_y\geq 2$ cm is set for the azimuthal wavelength. Thus, we conclude that from Eq. (1) the parallel coupling dominates the $\vec{E}\times\vec{B}$ coupling. Phase-velocity directions of the two daughter waves were determined either by inserting an additional length of transmission line at the reference side of the interferometer, or by using a boxcar integrator (applicable only for the ion-acoustic wave). As expected, the decay waves

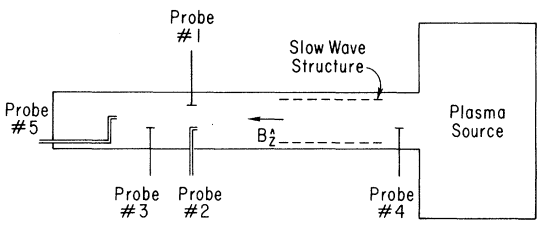

FIG. 1. Schematic of experimental setup.

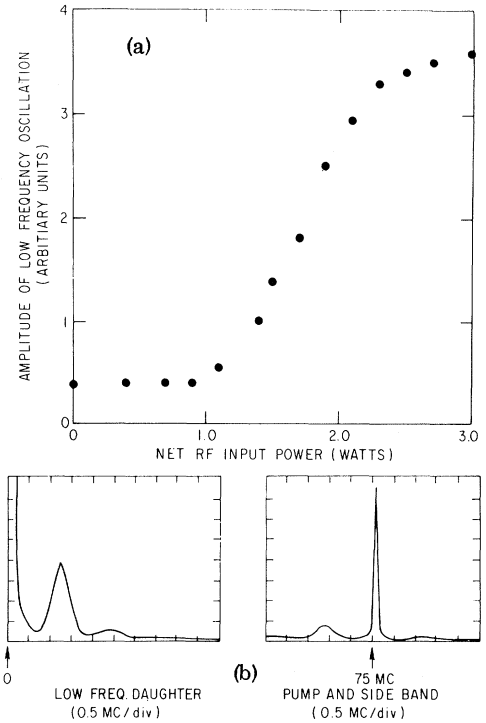

FIG. 2. (a) Determination of parametric decay threshold. (b) Parametric decay spectrum (linear sensitivity).

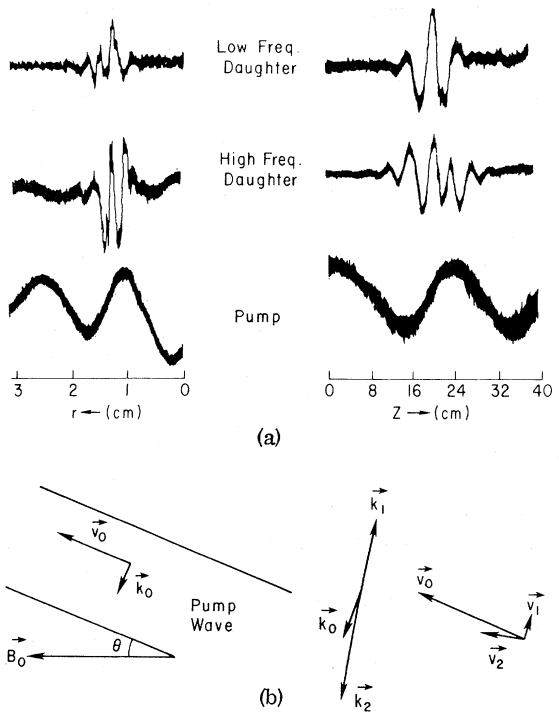

FIG. 3. (a) Radial and axial interferograms of the pump and the decay waves. (b) $\vec{k}$-vector diagram and group velocities constructed from the interferograms.

propagated nearly in opposite directions, thus satisfying the $\vec{k}$-matching condition. The $\vec{k}$-vector diagram is shown in Fig. 3(b). From the measured frequencies and wavelengths, the low-frequency decay wave was found to be an ion-acoustic wave ($\omega \simeq kC_s \gg \omega_{ci}$) which propagated nearly perpendicularly to the pump resonance cone. The high-frequency decay wave was identified to be an electrostatic electron plasma wave which obeyed the dispersion relation of Eq. (2) and it propagated along the pump wave packet. This is shown in the $\vec{k}$-vector diagram as well as in Fig. 4(a) where axial interferometer traces at various radial positions are displayed. The interferograms indicate that the sideband propagates along a conical trajectory and that the cone angle is nearly the same as the pump.

A different way to verify the effect of convective loss is to use the reference probe to launch a test wave near 1 MHz. To distinguish the test wave from the decay wave, the test wave was chopped and detected by a lock-in amplifier. It was found that the test-wave energy followed the conical trajectory of the pump as shown in Fig. 4(b). This indicates that test waves following the pump trajectory are amplified.

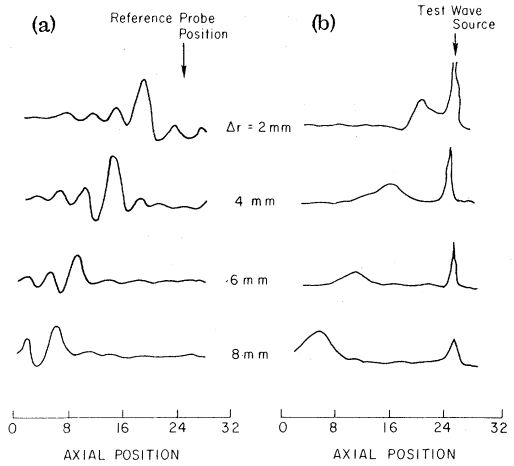

FIG. 4. (a) Axial interferograms of the sideband with the reference probe at $r = 1.0$ cm. The radial position of the axial probe was varied from 1.2 to 1.8 cm. (b) Test wave amplitude measured by the axial probe at various radial positions.

To determine the threshold fields, a calibrated double-tip probe was used. The measured threshold field was about 3.5 V/cm, slightly above the collisional threshold due to parallel coupling (~2 V/cm) and much higher that that due to $\vec{E}\times\vec{B}$ coupling (~0.4 V/cm). $\vec{E}\times\vec{B}$-coupled decay did not occur because of the convective loss in the finite-extent pump field. For the parallel-coupled decay, if the pump wave follows a single resonance-cone trajectory, it requires $E_{0x} \sim 23$ V/cm in order to satisfy Eq. (4). On the other hand, in the region where trajectories of the two resonance cones intersect, E_{0x} is a standing wave in the x direction and thus the decay waves have components $\pm V_{1x}, \pm V_{2x}$ so that convective losses are essentially eliminated. Thus substantial growth is expected only in such regions and this is in agreement with experimental observations. When the pump frequency and wavelength were varied, it was found that the decay occurred at higher threshold for lower pump frequency and shorter wavelength. At higher densities ($n > 5\times 10^{10}/\mathrm{cm}^3$), $\vec{E}\times\vec{B}$-coupled decay occurred and the sideband no longer followed the resonance cone trajectory of the pump. Details of these data will be published in a separate paper. Because of severe electron Landau damping and limited length of the plasma column, no data can be obtained with $\omega_0 \sim \omega_{pi}$.

In conclusion, we have verified experimentally that in the regime $\omega_{pi} \ll \omega_0 \ll \omega_{pe} \lesssim \omega_{ce}$, $T_e \gg T_i$, parametric coupling due to the parallel drift can compete with or even dominate over the $E\times B$

coupling during resonant decay of electron plasma waves. These results tend to corroborate recent theoretical predictions made for lower hybrid heating of tokamaks,[4,6] namely, that parametric instabilities driven by $\vec{E}\times\vec{B}$ coupling due to the finite-extent slow wave will be effectively stabilized in the region $\omega_0 \geq 2\omega_{pi}$.

One of the authors (K.L.W.) wishes to thank Dr. F. J. Paoloni for his assistance on the design of the rf transformer used in this experiment. Helpful discussions with Dr. P. K. Kaw and Mr. M. Ono are gratefully appreciated. This work was supported by the U. S. Department of Energy, Contract No. EY-76-C-02-3073.

[a]Present address: California Institute of Technology, Pasadena, Calif. 91109.

[1]T. H. Stix, Phys. Rev. Lett. 15, 878 (1965); V. E. Golant, Zh. Tekh. Fiz. 41, 2492 (1971) [Sov. Phys. Tech. Phys. 16, 1980 (1973)].

[2]M. Porkolab *et al.*, Phys. Rev. Lett. 38, 230 (1977).

[3]M. Porkolab, Phys. Fluids 17, 1432 (1974).

[4]M. Porkolab, to be published.

[5]R. L. Berger and F. W. Perkins, Phys. Fluids 19, 406 (1976).

[6]R. L. Berger, L. Chen, and F. W. Perkins, Princeton Plasma Physics Laboratory Report No. PPPL-1307, 1976 (unpublished).

[7]M. Porkolab and R. P. H. Chang, Phys. Fluids 13, 2054 (1970), see Eq. (16); D. Pesme *et al.*, Phys. Rev. Lett. 31, 203 (1973), see Eq. (8).

[8]S. Bernabei *et al.*, Princeton Plasma Physics Laboratory Report No. PPPL-1288, 1976 (unpublished), and Phys. Rev. Lett. 34, 866 (1975).

[9]W. M. Hooke and S. Bernabei, Phys. Rev. Lett. 29, 1218 (1972).

[10]R. P. H. Chang and M. Porkolab, Phys. Rev. Lett. 31, 1241 (1973), and 32, 1227 (1974).

[11]T. K. Chu, S. Bernabei, and R. W. Motley, Phys. Rev. Lett. 31, 211 (1973).

[12]M. Porkolab, V. Arunasalam, and N. C. Luhman, Plasma Phys. 17, 405 (1975).

[13]R. W. Boswell, in *Proceedings of the Seventh European Conference on Controlled Fusion and Plasma Physics, Lausanne* (Centre de Recherches en Physique des Plasma, 1975), p. 175.

[14]R. R. Weynants, P. Javel, and G. Muller, in *Proceedings of the Topical International Conference on Theoretical and Experimental Aspects of Heating of Toroidal Plasmas, Grenoble* (Commissariat à l'Energie Atomique, Paris, 1976), Vol. II, p. 421.

[15]W. Gekelman and R. L. Stenzel, Rev. Sci. Instrum. 46, 1386 (1975).

[16]P. Bellan and M. Porkolab, Phys. Rev. Lett. 34, 124 (1975).

Evidence for Electronic Ferromagnetism in Superfluid ^{3}He-*A*

D. N. Paulson and J. C. Wheatley
Department of Physics, University of California at San Diego, La Jolla, California 92093
(Received 19 December 1977)

Experiments on ^{3}He-*A* show that the orientation of the orbital field $\hat{l}$ depends on the *sign* of the applied magnetic field, as if there were a ferromagnetic magnetization along $\hat{l}$ estimated by $|(10\ \mathrm{mG})(1-T/T_c)\chi_N|$, in agreement with a recent prediction by Leggett.

The orbital-ordering vector $\hat{l}$ in superfluid liquid[1,2] ^{3}He-*A* can be conceived either as that direction along which no correlated pairs have their relative linear momentum or possibly as the direction of the relative angular momentum of the correlated pairs. Changes in the direction of $\hat{l}$ can be measured with great sensitivity[3] using the anisotropy of zero-sound attenuation with respect to the angle between $\hat{l}$ and $\vec{q}$, the sound propagation vector. In the presence of very weak superfluid flow fields $\vec{v}_s$ and for open geometries which diminish the effect of boundaries on the orientation of $\hat{l}$, the direction of $\hat{l}$ can be controlled efectively by weak magnetic fields via (at least) the nuclear magnetic susceptibility anisotropy energy (coupling the magnetic field to the spin-ordering vector $\hat{d}$ which is maintained parallel to $\hat{l}$ by the strong coherent nuclear magnetic dipolar energy). Under such rather ideal conditions, necessary because of the smallness of the present effect, we have discovered that the orientation of the average field of $\hat{l}$ for ^{3}He-*A* in a zero-sound cell depends on the *sign* of the applied magnetic field $\vec{H}_{ext}$: A change from $\vec{H}_{ext}$ to $-\vec{H}_{ext}$ changes the average orientation of $\hat{l}$ in a way which depends both on temperature and on the texture (field of $\hat{l}$) and which cannot be explained as a simple consequence of field rotation due to the residual trapped and therefore nonreversing magnetic fields in our apparatus. The magnitude of